

Upregulation of matrix metalloproteinase 9 (MMP9)/tissue inhibitor of metalloproteinase 1 (TIMP1) and MMP2/TIMP2 ratios may be involved in lipopolysaccharide-induced acute lung injury

Guobing Chen^{1,2,*} , Dandan Ge^{1,4,*},
Bizhen Zhu¹, Huixuan Shi¹ and Qilin Ma^{2,3}

Abstract

Objective: This study aimed to examine the changes and significance of matrix metalloproteinase 9 (MMP9), MMP2, tissue inhibitor of metalloproteinase 1 (TIMP1), and TIMP2 in rats with lipopolysaccharide (LPS)-induced acute lung injury (ALI).

Methods: Wistar rats were randomly divided into a control group (injected with saline) and an ALI group (injected with LPS), then subdivided into four time points (2, 6, 12, and 24 hours). Serum tumor necrosis factor alpha and interleukin-6 levels were detected by ELISA to investigate the inflammatory reaction after LPS injection. The degree of ALI was determined by hematoxylin–eosin staining of lung tissue, the lung wet/dry weight ratio, and pulmonary permeability index. Changes in lung MMP and TIMP protein and mRNA levels were detected by western blotting and quantitative real-time polymerase chain reaction.

¹Department of Pediatrics, The First Affiliated Hospital of Xiamen University, Xiamen, Fujian, China

²School of Medicine, Xiamen University, Xiamen, Fujian, China

³Department of Neurology, The First Affiliated Hospital of Xiamen University, Xiamen, Fujian, China

⁴Pediatric Key Laboratory of Xiamen, Xiamen, Fujian, China

*These authors contributed equally to this work.

Corresponding author:

Qilin Ma, Department of Neurology, The First Affiliated Hospital of Xiamen University, 55 Zhenhai Road, Siming District, Xiamen, Fujian, 361003, China.

Email: qilinma@yeah.net



Results: Changes in the ratios of MMP9/TIMP1 and MMP2/TIMP2 were consistent with and strongly positively associated with the lung wet/dry weight ratio, the pulmonary permeability index, and serum tumor necrosis factor alpha and interleukin-6 levels in the ALI group.

Conclusion: ALI induced by LPS may be related to upregulation of MMP9/TIMP1 and MMP2/TIMP2 ratios.

Keywords

Matrix metalloproteinase (MMP), tissue inhibitor of metalloproteinase (TIMP), acute lung injury, lipopolysaccharide, rat, lungs

Date received: 22 September 2019; accepted: 8 March 2020

Introduction

Acute lung injury (ALI) is a diffuse lung injury caused by a variety of factors.^{1,2} ALI mainly is caused by lung infection, sepsis, and foreign body inhalation,³ with clinical manifestations of progressive hypoxia and dyspnea.^{4,5} The pathogenesis of ALI has not yet been fully determined, but release of lipopolysaccharide (LPS) from bacterial infection is thought to be the main cause.^{6,7} ALI is associated with inflammatory cell infiltration of lung tissues, an impaired alveolar–capillary membrane, and increased permeability of the microvasculature, leading to exudative pulmonary edema,^{8,9} and ultimately causing dysfunction of lung ventilation. Alveolar–capillary membrane injury is the main cause of ALI.^{10,11}

The extracellular matrix (ECM) is the main structural component of the alveolar–capillary membrane.^{12,13} Previous studies have shown that matrix metalloproteinases (MMPs) and tissue inhibitors of matrix metalloproteinases (TIMPs) are the most important enzyme systems involved in metabolism of the ECM.^{14,15} Under normal circumstances, if the lung MMP/TIMP ratio is balanced, synthesis and degradation of the ECM are in a state of dynamic equilibrium.¹⁶ Therefore, balance of the MMP/TIMP ratio

might be important for lung tissue injury and repair. However, little is known about this possible situation.

In this study, we examined changes in MMP9, MMP2, and their inhibitors TIMP1 and TIMP2 in rats with LPS-induced ALI. We aimed to understand the relationship between ALI and changes in lung MMP/TIMP ratios.

Materials and methods

Reagents

The cDNA synthesis kit (cat. no. KR116-02) was purchased from Tiangen Biotech Co., Ltd. (Beijing, China). Goat anti-rat MMP2 (cat. no. AF1488-SP), TIMP1 (cat. no. AF580-SP), and mouse anti-rat β -actin antibodies (cat. no. MAB8929-SP) were purchased from R&D Biotech Co., Ltd. (San Diego, CA, USA). Mouse anti-rat MMP9 (cat. no. NBP2-13173SS) and TIMP2 antibodies (cat. no. NBP1-42375) were purchased from Novus Biologicals Inc. (Littleton, CO, USA). Goat anti-mouse secondary antibody (cat. no. BA1050) and rabbit anti-goat secondary antibody (cat. no. BA1060) were obtained from Boster Biological Technology Co., Ltd. (Wuhan, China).

Animals

Specific pathogen-free male Wistar rats were purchased from Charles River Experimental Animal Co., Ltd. (Beijing, China) and raised in the Xiamen University Laboratory Animal Center (license number: SYXK [Min] 2018-0010). The rats were housed 1 week before the start of experiment under standard laboratory conditions at a temperature of $22 \pm 2^\circ\text{C}$, humidity of $50\% \pm 10\%$, and a 12/12-hour light/dark cycle with food and water ad libitum.¹⁷ The research followed internationally recognized guidelines on animal welfare, as well as local and national regulations.

ALI modeling and grouping

Forty-eight 2-month-old male Wistar rats (180 ± 200 g) were randomly divided into the normal control (NC) and ALI groups. The ALI model was prepared by intravenous injection of 5 mg/kg LPS (*Escherichia coli* 055: B5, cat. no. L2880; Sigma-Aldrich, St. Louis, MO, USA).^{18,19} The NC group was injected with the same amount of saline. The two groups were further divided into subgroups of 2, 6, 12, and 24 hours with six rats for each time point. The rats were anesthetized via intraperitoneal injection with 2.25% pentobarbital sodium (45 mg/kg, WS20060401; Sinopharm Chemical Reagent Co., Ltd., Beijing, China).²⁰ Blood, lung tissue, and bronchoalveolar lavage fluid (BALF) specimens were collected at each designated time point. All animal procedures were carried out at the Xiamen University Laboratory Animal Center and approved by the Ethics Committee of the First Affiliated Hospital of Xiamen University.

Detection of serum tumor necrosis factor alpha and interleukin-6 using ELISA

The rats were anesthetized followed by collection of 3 mL of blood from the

abdominal aorta. After centrifuging the blood samples at $3500 \times g$ for 10 minutes, the supernatant was collected. Tumor necrosis factor alpha (TNF- α) (Quantikine ELISA kit, cat. no. RTA00; R&D Biotech Co., Ltd.) and interleukin (IL)-6 (cat. no. RK00020; ABclonal, Inc., Boston, MA, USA) levels were measured according to ELISA procedures as described by the manufacturers to investigate the inflammatory reaction in rats.

Hematoxylin–eosin staining

Small pieces of upper left lung tissue were fixed in 4% formaldehyde for 24 hours, followed by conventional paraffin embedding and tissue sectioning at 5- μm thickness.²¹ The tissue sections were stained with hematoxylin–eosin (ZhuHai Besso Biotechnology Co., Ltd., ZhuHai, China). Morphological changes in lung tissue were observed under a light microscope to observe the degree of lung injury.

Lung wet/dry weight ratio

Surfaces of small pieces of lower left lung tissue were dried using paper towels and then the tissues were immediately weighed to record the wet weight. The lung tissues were then placed in an incubator at 60°C for 72 hours to obtain the dry weight, and the weight was recorded as the dry weight. The wet and dry weights were used to calculate the wet/dry weight (W/D) ratio of the lungs to determine the severity of edema of lung tissue.²²

Detection of the pulmonary permeability index

Detection of protein was achieved by a bicinchoninic acid protein quantitative kit (cat. no. PP0101; Tiangen Biotech Co., Ltd.). The absorbance was measured at 562 nm in wavelength with a multi-function microplate reader (Modulus photometer,

Turner Biosystems Inc., Sunnyvale, CA, USA) and a protein standard curve was drawn. Bronchoalveolar lavage was performed three times using 1 mL of phosphate-buffered saline per lavage and 90% recovery. The protein content of BALF and plasma were calculated according to the absorbance values. To determine the extent of the lung injury, the pulmonary permeability index (PPI) was calculated using the following equation: $PPI = \text{BALF protein content} / \text{plasma protein content}$.²³

Measurement of MMP and TIMP mRNA expression levels

Approximately 50 mg of right middle lobe lung tissue was used for total RNA extraction (cat. no. LS1040; Promega, Madison, WA, USA) using TRIzol (cat. no. DP405-02; Tiangen Biotech Co.). After analyzing the total RNA concentration and purity, β -actin was used as an internal control for real-time quantitative polymerase chain reaction ([qPCR] cat. no. A6002; Promega). PCR primers were synthesized by Sangon Biotech Co., Ltd. (Shanghai, China). The forward and reverse primer sequences for MMP2, MMP9, TIMP1, TIMP2, and β -actin are shown in Table 1. The qPCR conditions were preliminary denaturation at 95°C for 2 minutes, followed by 40 cycles of denaturation at 95°C for 15 seconds, annealing at 58°C for 34 seconds, and elongation at 72°C for 1 minute, followed by a final elongation

step at 72°C for 5 minutes. This was performed on a CFX96 Touch Real-Time PCR Detection System (BioRad, Hercules, CA, USA). PCR products were separated on 1% agarose gels and visualized using ethidium bromide staining and ultraviolet light to verify the product sizes. Glyceraldehyde 3-phosphate dehydrogenase was used as the loading control for normalization of the data. Data from qPCR were analyzed using the $2^{-\Delta\Delta C_t}$ method.²⁴

MMP and TIMP protein expression levels

Approximately 50 mg of lower right lung tissue samples were collected from the different groups of rats, followed by washing, homogenization, and lysing. After conventional protein extraction from lung tissue, total protein concentrations were measured. A total of 30 μ g of total protein was then added to a one third volume of 4 \times sodium dodecyl sulfate-polyacrylamide gel electrophoresis sample buffer (cat. no. 30166428; Sinopharm Chemical Reagent Co., Ltd.), the protein sample was boiled for 10 minutes, and the protein was separated by sodium dodecyl sulfate-polyacrylamide gel electrophoresis. After transferring the separated proteins onto a polyvinylidene fluoride membrane (cat. no. IPVH00010; Emd Millipore BioTechniques Co., Ltd., Billerica, MA, USA), the protein blots were prepared according to conventional procedures of western blot analysis. After developing the protein blots in

Table 1. Primer sequences for real-time quantitative polymerase chain reaction analyses.

Gene	Forward primer	Reverse primer
MMP2	ACCGAGGATTATGACCGGGA	GCTGGTGCAGCTCTCATACT
MMP9	TGGATGGTTATCGCTGGTG	AAGACGCACATCTCTCCTGC
TIMP1	ACAGCTTTCTGCAACTCGGA	CGGAAACCTGTGGCATTTC
TIMP2	CGAGAAGGAGGTGGATTCCG	CCGCCTTCCCTGCAATTAGA
β -actin	TGTCACCAACTGGGACGATA	GGGGTGTGAAGGTCTCAA

MMP2, matrix metalloproteinase 2; MMP9, matrix metalloproteinase 9; TIMP1, tissue inhibitor of metalloproteinase 1; TIMP2, tissue inhibitor of metalloproteinase 2.

electrochemiluminescence reagent (cat. no. K-12043-D10; Advansta Inc., Menlo Park, CA, USA), the absorbance values of protein bands were scanned by a gel imaging system (LI-COR, Lincoln, NE, USA) to calculate the relative protein expression levels of MMPs and TIMPs according to the ratios of MMP and TIMP absorbance to β -actin absorbance.

Statistical analyses

SPSS version 21.0 software (IBM Corp., Armonk, NY, USA) was used for statistical analysis. Each measurement was presented as the mean \pm standard deviation. The independent sample t-test was used for comparison between groups. One-way ANOVA was used for comparison within groups. Pearson's correlation analysis was used for the relevant trend variables. $P < 0.05$ was considered statistically significant.

Results

Changes in the serum inflammatory factors TNF- α and IL-6

Serum TNF- α and IL-6 levels were significantly higher at 2 hours in the ALI group compared with the NC group (both $P < 0.05$), peaked at 12 hours (both $P < 0.05$), and partially recovered at 24 hours (Figure 1).

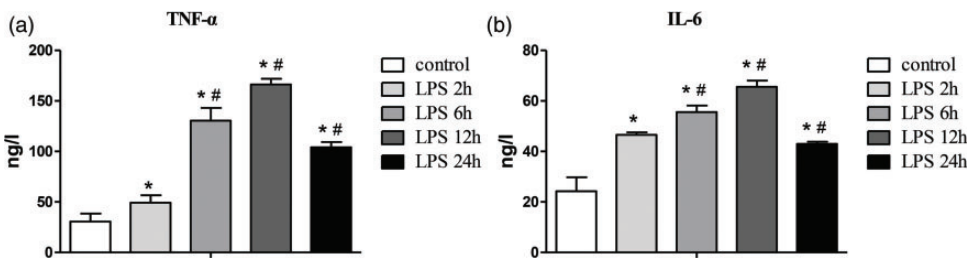


Figure 1. Changes in TNF- α and IL-6 levels in response to the degree of inflammatory reaction after LPS injection. (a) Changes in TNF- α levels; (b) changes in IL-6 levels. LPS 2h, 6h, 12h, and 24h indicate 2, 6, 12, and 24 hours after LPS injection in the acute lung injury group, respectively. Data are shown as mean \pm standard deviation ($n = 6$ per group). * $P < 0.05$ vs. control, # $P < 0.05$ vs. LPS 2h. Control, normal control group; TNF- α , tumor necrosis factor alpha; IL-6, interleukin-6; LPS, lipopolysaccharide.

Changes in indicators related to ALI

The lung W/D ratio and PPI in the ALI group were significantly higher than those in the NC group at all time points (all $P < 0.05$), with a peak at 12 hours (Figure 2).

Hematoxylin-eosin staining of lung tissue showed alveolar and interstitial edema, inflammatory cell infiltration, and spotted hemorrhages on the surface of lung tissue at 2 hours after LPS injection. These phenomena were more obvious at 6 and 12 hours and were improved at 24 hours. However, bronchial, alveolar, and vascular structures in the NC group were normal (Figure 3).

Changes in lung MMP and TIMP mRNA and protein expression

Western blotting and qPCR showed that MMP2 and MMP9 mRNA and protein expression gradually increased over time following LPS injection, mostly peaked at 12 hours, and recovered at 24 hours. TIMP1 and TIMP2 expression in the ALI group was significantly higher (all $P < 0.05$) than that in the NC group at all time points, except at 2 hours for TIMP1. MMP9/TIMP1 and MMP2/TIMP2 ratios were significantly higher at each time point in the ALI group (except for at 2 hours for the MMP2/TIMP2 ratio) compared with

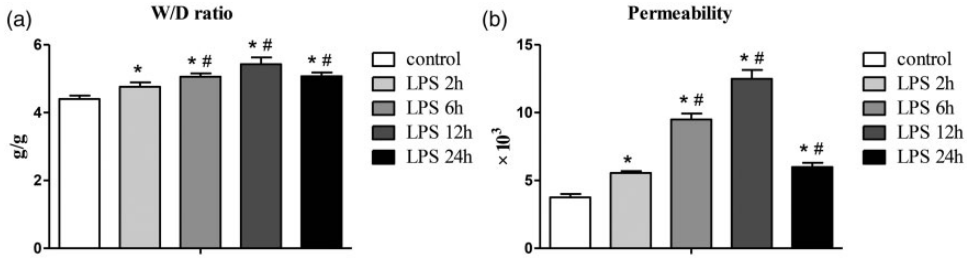


Figure 2. Lung W/D ratio and changes in permeability in each group. W/D ratio and permeability reflect changes in pulmonary edema and the degree of lung injury, respectively. (a) Changes in the W/D ratio; (b) changes in the lung permeability index. LPS 2h, 6h, 12h, and 24h indicate 2, 6, 12, and 24 hours after LPS injection in the acute lung injury group, respectively. Data are shown as mean \pm standard deviation ($n = 6$ per group). * $P < 0.05$ vs. control, # $P < 0.05$ vs. LPS 2h. LPS, lipopolysaccharide.

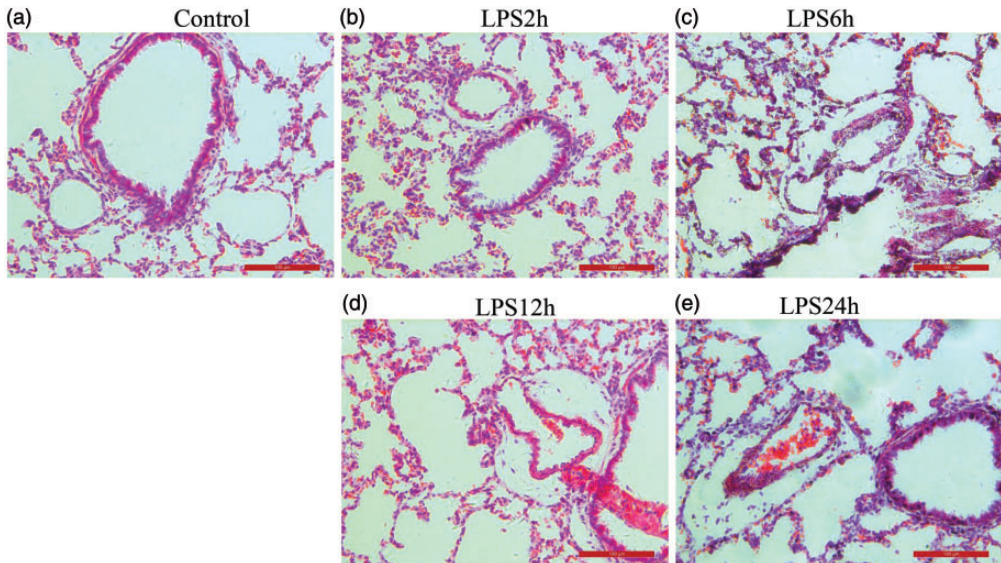


Figure 3. Morphological changes in lung tissue sections stained with hematoxylin–eosin among the groups (200 \times magnification). (a) Normal control group; (b–e) 2, 6, 12, and 24 hours after LPS injection groups. LPS, lipopolysaccharide.

the NC group, and peaked at 12 hours (all $P < 0.05$) (Figure 4).

Discussion

ALI is a relatively common critical illness in children, with a high mortality rate, and survivors often experience lung structural disorders and dysfunction.²⁵ The

pathogenesis of ALI has not been fully determined. When Gram-negative bacteria infect the body, they release LPS to induce the release of inflammatory cytokines, such as TNF- α and IL-6.^{26,27} This causes accumulation of neutrophils in lung tissue, destruction of alveolar epithelial structure, damage to the ECM, and exudative pulmonary edema.^{28,29}

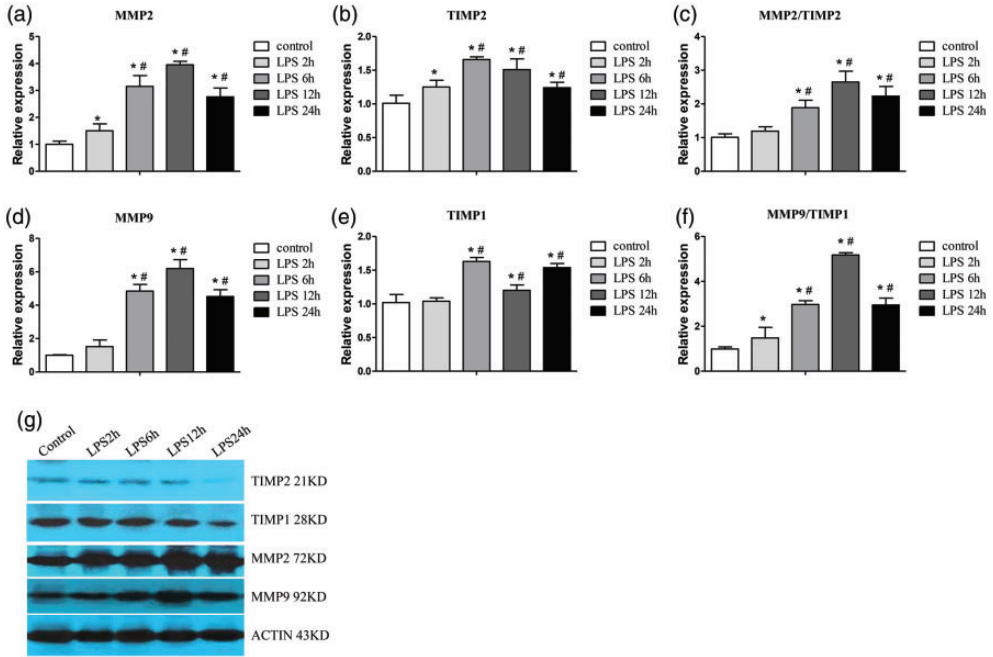


Figure 4. Lung MMP and TIMP mRNA and protein expression. Changes in MMP2 (a), TIMP2 (b), MMP2/TIMP2 (c), MMP9 (d), TIMP1 (e), and MMP9/TIMP1 (f) in all groups treated with or without LPS. (g) Protein expression in each group as detected by western blotting. LPS 2h, 6h, 12h, and 24h indicate 2, 6, 12, and 24 hours after LPS injection in the acute lung injury group, respectively. Data are shown as mean \pm standard deviation ($n = 6$ per group). * $P < 0.05$ vs. control, # $P < 0.05$ vs. LPS 2h. Control, normal control group; MMP, matrix metalloproteinase; TIMP, tissue inhibitor of metalloproteinase; LPS, lipopolysaccharide

In the current study, the rats developed irritability and cyanosis 2 hours after LPS injection, and serum TNF- α and IL-6 levels were significantly higher compared with NC rats. Additionally, these rats had swollen alveolar epithelial cells, interstitial edema, and a significantly higher lung W/D ratio and PPI compared with the NC group. These findings suggested that injection of LPS resulted in ALI in rats and inflammatory edema in the alveoli. The lung injury gradually became aggravated over time, and peaked at 12 hours after LPS injection. After this time, with a decrease in serum inflammatory cytokines, the indices of lung injury were gradually reduced.

The lung ECM is the main component of the alveolar-capillary membrane and is a dynamic network of macromolecules, such

as collagen, proteoglycans, and glycoproteins. The ECM not only exerts mechanical support and connection between cells, but also serves as a bridge between cells. The ECM plays an important role in maintaining normal tissue structure and function, as well as cell growth and differentiation.^{16,30,31} Previous studies have shown that ECM metabolic disorders are involved in the pathophysiological process of ALI and chronic lung injury.^{32,33}

MMPs are a class of proteolytic enzymes that rely on metal ions, such as zinc and calcium ions. MMPs use ECM components as a hydrolysis substrate to maintain pathophysiological processes, such as normal transformation of ECM, cell migration and proliferation, tissue remodeling and repair, and the inflammatory response.^{34,35}

To date, more than 20 members of the MMP family have been discovered, and among them, MMP2 and MMP9 can degrade the main structural components of the basement membrane, such as type IV collagen. MMPs play an important role in degradation and remodeling of the alveolar–capillary membrane and maintenance of the integrity of the basement membrane.^{36,37}

Among the TIMPs, TIMP1 is an MMP9-specific tissue inhibitor, and TIMP2 is an MMP2-specific tissue inhibitor.³⁸ The cysteine residues in the N-terminal domain of TIMPs bind to the zinc ion active center of MMPs to form MMP–TIMP complexes in a 1: 1 ratio. This process blocks binding of MMPs to ECM substrates, effectively inhibiting the activity of MMPs, and participates in regulation of synthesis and degradation of the ECM.³⁹

Under normal circumstances, the proportion of MMPs/TIMPs in the lung and synthesis and degradation of the ECM are in a state of dynamic equilibrium. Once this balance is disturbed, it may cause an increase in degradation of the ECM, which leads to destruction of normal tissue structure and aggravation of lung injury. Conversely, if degradation of the ECM is reduced, ECM that is accumulated in the stroma may lead to fibrosis of lung tissue.⁴⁰

Our study showed that the LPS-induced ALI in rats gradually increased mRNA and protein expression of MMP2 and MMP9 with time. This increase peaked at 12 hours and recovered at 24 hours, and caused damage of the ECM in the alveolar–capillary membrane. Additionally, the corresponding tissue inhibitors, TIMP1 and TIMP2, were increased to varying degrees, which suggested that the body also underwent limited tissue repair. Our study also showed that changes in the ratios of MMP9/TIMP1 and MMP2/TIMP2 were consistent with and strongly positively associated with the lung W/D

ratio, PPI, and TNF- α and IL-6 levels in the ALI group. These results indicated that LPS caused ALI through upregulation of MMP/TIMP ratios, increased permeability of the alveolar–capillary membrane, and induced inflammatory edema in the alveoli. Therefore, our model represented clinical manifestations of progressive hypoxemia and respiratory distress.

In summary, the imbalance between MMPs and TIMPs leads to an imbalance of ECM metabolism, which in turn affects development and progression of lung injury. Inhibition of MMP2 and MMP9 activity may reduce degradation of the ECM and alleviate lung injury, which could be a new direction for treating ALI. Development of MMP inhibitors with high selectivity and high bioavailability according to their mechanism may provide an important research direction and may also become a new entry point for preventing ALI and treatment strategies for ALI.

Declaration of conflicting interest

The authors declare that there is no conflict of interest.

Funding

This study was supported by the Xiamen Science and Technology Bureau (Grant no. 3502Z20154013) and Xiamen City Science and Technology Major Special Project: Xiamen City major disease first aid technology research and first aid network body special (Grant no. 3502Z20171005-20170801).

ORCID iD

Guobing Chen  <https://orcid.org/0000-0002-5281-3105>

References

1. Schmidt GA. Managing acute lung injury. *Clin Chest Med* 2016; 37: 647–658.
2. Hughes KT and Beasley MB. Pulmonary manifestations of acute lung injury: more

- than just diffuse alveolar damage. *Arch Pathol Lab Med* 2017; 141: 916–922.
3. Butt Y, Kurdowska A and Allen TC. Acute lung injury: a clinical and molecular review. *Arch Pathol Lab Med* 2016; 140: 345–350.
 4. Confalonieri M, Salton F and Fabiano F. Acute respiratory distress syndrome. *Eur Respir Rev* 2017; 26: 160116.
 5. Liang Y, Yang N, Pan G, et al. Elevated IL-33 promotes expression of MMP2 and MMP9 via activating STAT3 in alveolar macrophages during LPS-induced acute lung injury. *Cell Mol Biol Lett* 2018; 23: 52.
 6. Lei J, Wei Y, Song P, et al. Cordycepin inhibits LPS-induced acute lung injury by inhibiting inflammation and oxidative stress. *Eur J Pharmacol* 2018; 818: 110–114.
 7. Wang X, Zhang L, Duan W, et al. Anti-inflammatory effects of triptolide by inhibiting the NF- κ B signalling pathway in LPS-induced acute lung injury in a murine model. *Mol Med Rep* 2014; 10: 447–452.
 8. Fanelli V and Ranieri VM. Mechanisms and clinical consequences of acute lung injury. *Ann Am Thorac Soc* 2015; 12: S3–S8.
 9. Ware LB and Herridge M. Acute lung injury. *Semin Respir Crit Care Med* 2013; 34: 439–440.
 10. Nova Z, Skovierova H and Calkovska A. Alveolar-capillary membrane-related pulmonary cells as a target in endotoxin-induced acute lung injury. *Int J Mol Sci* 2019; 20: pii: E831.
 11. Zeng Z, Gong H, Li Y, et al. Upregulation of miR-146a contributes to the suppression of inflammatory responses in LPS-induced acute lung injury. *Exp Lung Res* 2013; 39: 275–282.
 12. Roychaudhuri R, Hergrueter AH, Polverino F, et al. ADAM9 is a novel product of polymorphonuclear neutrophils: regulation of expression and contributions to extracellular matrix protein degradation during acute lung injury. *J Immunol* 2014; 193: 2469–2482.
 13. Nkyimbeng T, Ruppert C, Shiomi T, et al. Pivotal role of matrix metalloproteinase 13 in extracellular matrix turnover in idiopathic pulmonary fibrosis. *PLoS One* 2013; 8: e73279.
 14. Jabłońska-Trypuć A, Matejczyk M and Rosochacki S. Matrix metalloproteinases (MMPs), the main extracellular matrix (ECM) enzymes in collagen degradation, as a target for anticancer drugs. *J Enzyme Inhib Med Chem* 2016; 31: 177–183.
 15. Higueta-Castro N, Nelson MT, Shukla V, et al. Using a novel microfabricated model of the alveolar-capillary barrier to investigate the effect of matrix structure on atelectrauma. *Sci Rep* 2017; 7: 11623.
 16. Cui N, Hu M and Khalil RA. Biochemical and biological attributes of matrix metalloproteinases. *Prog Mol Biol Transl Sci* 2017; 147: 1–73.
 17. Li L, Zhang YG, Tan YF, et al. Tanshinone II is a potent candidate for treatment of lipopolysaccharide-induced acute lung injury in rat model. *Oncol Lett* 2018; 15: 2550–2554.
 18. Jiang X, Yu M, Zhu T, et al. Kcnq1ot1/miR-381-3p/ETS2 axis regulates inflammation in mouse models of acute respiratory distress syndrome. *Mol Ther Nucleic Acids* 2019; 19: 179–189.
 19. Coimbra R, Melbostad H, Loomis W, et al. LPS-induced acute lung injury is attenuated by phosphodiesterase inhibition: effects on proinflammatory mediators, metalloproteinases, NF- κ B, and ICAM-1 expression. *J Trauma* 2006; 60: 115–125.
 20. Chen L, Zheng Q, Chen X, et al. Low-frequency ultrasound enhances vascular endothelial growth factor expression, thereby promoting the wound healing in diabetic rats. *Exp Ther Med* 2019; 18: 4040–4048.
 21. Slaoui M, Bauchet AL and Fiette L. Tissue sampling and processing for histopathology evaluation. *Methods Mol Biol* 2017; 1641: 101–114.
 22. Qin L, Tan HL, Wang YG, et al. Astragalus membranaceus and *Salvia miltiorrhiza* ameliorate lipopolysaccharide-induced acute lung injury in rats by regulating the Toll-like receptor 4/nuclear factor- κ B signaling pathway. *Evid Based Complement Alternat Med* 2018; 2018: 3017571.
 23. Caruso JM, Xu DZ, Lu Q, et al. The female gender protects against pulmonary injury after trauma hemorrhagic shock. *Surg Infect (Larchmt)* 2001; 2: 231–240.

24. Huang L, Ding W, Wang MQ, et al. Tanshinone IIA ameliorates non-alcoholic fatty liver disease through targeting peroxisome proliferator-activated receptor gamma and toll-like receptor 4. *J Int Med Res* 2019; 47: 5239–5255.
25. Nelson AR, Fingleton B, Rothenberg ML, et al. Matrix metalloproteinases: biologic activity and clinical implications. *J Clin Oncol* 2000; 18: 1135–1149.
26. Meng J, Zou Y, Chen J, et al. sTLR4/sMD-2 complex alleviates LPS-induced acute lung injury by inhibiting pro-inflammatory cytokines and chemokine CXCL1 expression. *Exp Ther Med* 2018; 16: 4632–4638.
27. Aggarwal NR, King LS and D'Alessio FR. Diverse macrophage populations mediate acute lung inflammation and resolution. *Am J Physiol Lung Cell Mol Physiol* 2014; 306: L709–L725.
28. Lu Y, Jiang Y, Ling L, et al. Beneficial effects of *Houttuynia cordata* polysaccharides on “two-hit” acute lung injury and endotoxic fever in rats associated with anti-complementary activities. *Acta Pharm Sin B* 2018; 8: 218–227.
29. Jung JY, Kim HS, Roh MR, et al. The effect of imiquimod on matrix metalloproteinases and tissue inhibitors of metalloproteinases in malignant melanoma cell invasion. *Ann Dermatol* 2014; 26: 363–373.
30. Davey A, McAuley DF and OKane CM. Matrix metalloproteinases in acute lung injury: mediators of injury and drivers of repair. *Eur Respir J* 2011; 38: 959–970.
31. Hendrix AY and Kheradmand F. The role of matrix metalloproteinases in development, repair, and destruction of the lungs. *Prog Mol Biol Transl Sci* 2017; 148: 1–29.
32. Levin M, Udi Y, Solomonov I, et al. Next generation matrix metalloproteinase inhibitors—Novel strategies bring new prospects. *Biochim Biophys Acta Mol Cell Res* 2017; 1864: 1927–1939.
33. Hirota N and Martin JG. Mechanisms of airway remodeling. *Chest* 2013; 144: 1026–1032.
34. Robert S, Gicquel T, Victoni T, et al. Involvement of matrix metalloproteinases (MMPs) and inflammasome pathway in molecular mechanisms of fibrosis. *Biosci Rep* 2016; 36: e00360.
35. Dimas G, Iliadis F and Grekas D. Matrix metalloproteinases, atherosclerosis, proteinuria and kidney disease: linkage-based approaches. *Hippokratia* 2013; 17: 292–297.
36. Xiao XG, Zu HG, Li QG, et al. Sivelestat sodium hydrate attenuates acute lung injury by decreasing systemic inflammation in a rat model of severe burns. *Eur Rev Med Pharmacol Sci* 2016; 20: 528–536.
37. Aschner Y, Zemans RL, Yamashita CM, et al. Matrix metalloproteinases and protein tyrosine kinases: potential novel targets in acute lung injury and ARDS. *Chest* 2014; 146: 1081–1091.
38. Barton AK, Shety T, Bondzio A, et al. Metalloproteinases and their tissue inhibitors in comparison between different chronic pneumopathies in the horse. *Mediators Inflamm* 2015: 569512.
39. Pietruszewska W, Bojanowska-Poźniak K and Kobos J. Matrix metalloproteinases MMP1, MMP2, MMP9 and their tissue inhibitors TIMP1, TIMP2, TIMP3 in head and neck cancer: an immunohistochemical study. *Otolaryngol Pol* 2016; 70: 32–43.
40. Piesiak P, Brzecka A, Kosacka M, et al. Concentrations of matrix metalloproteinase-9 and tissue inhibitor of metalloproteinases-1 in serum of patients with chronic obstructive pulmonary disease. *Pol Merkur Lekarski* 2011; 31: 270–273.